Geophysical Research Letters

RESEARCH LETTER
10.1029/2024GL113090

Is OSSO a Significant Contributor to the Unknown UV Absorber in Venus' Atmosphere?

Joanna V. Egan[1], Wuhu Feng[1,2], Alexander D. James[1], James Manners[3], Daniel R. Marsh[1,4], Sébastien Lebonnois[5], Franck Lefèvre[6], Aurélien Stolzenbach[6,7], and John M. C. Plane[1]

[1]School of Chemistry, University of Leeds, Leeds, UK, [2]NCAS, University of Leeds, Leeds, UK, [3]Met Office, Exeter, UK, [4]School of Physics and Astronomy, University of Leeds, Leeds, UK, [5]Laboratoire de Météorologie Dynamique, Sorbonne Université, ENS, PSL Research University, École Polytechnique, Institut Polytechnique de Paris, CNRS, Paris, France, [6]LATMOS, Sorbonne Université, UVSQ Paris-Saclay, CNRS, Paris, France, [7]Instituto de Astrofisica de Andalucia (IAA/CSIC), Granada, Spain

Abstract It has been proposed that two isomers of the SO dimer (*cis*- and *trans*-OSSO) are candidates for the unknown UV absorber in Venus' atmosphere because they have a good spectral match with the absorber, despite the low concentrations predicted by 1D photochemical models. Here OSSO chemistry (production from SO and loss by photolysis, thermal decomposition, and reaction with O and Cl) has been included in the photochemistry scheme of a 3D planetary climate model (PCM-Venus) along with sulfur injection due to meteoric ablation. 1D multiple scattering radiative transfer modeling is then used to predict the resulting top-of-the-atmosphere reflectance produced by OSSO. The modeled OSSO concentrations are shown to be ∼3 orders of magnitude too low to explain the observed absorbance levels, and the predicted ratio of the OSSO isomers provides an unsatisfactory match to the spectral shape of the unknown absorber.

Plain Language Summary Strong absorption is observable in Venus' atmosphere in the near-ultraviolet wavelength region. A combination of isomers of the SO dimer (OSSO) have previously been proposed as the cause of this absorption. Using 3D photochemical and dynamical atmospheric modeling, including state-of-the-art kinetics, we predict the concentration of OSSO in the Venusian atmosphere. Using radiative transfer modeling, we predict the effect the modeled concentration of OSSO would have on the observed Venusian reflectance and compare to published observations taken by the MASCS instrument on board the MESSENGER spacecraft in 2007. We find that the predicted OSSO concentration is too low to explain the observed absorption by a factor of 1000 and conclude that OSSO cannot be a major contributor to the unknown UV absorber on Venus.

Key Points:

- OSSO concentrations in the Venusian atmosphere are modeled to be three orders of magnitude too small to explain the Venusian unknown UV absorption
- The shape of the resulting UV absorption is a poor fit to the observed absorption
- This appears to rule out OSSO as a major contributor to the Venusian UV absorption

Supporting Information:

Supporting Information may be found in the online version of this article.

Correspondence to:

J. M. C. Plane,
j.m.c.plane@leeds.ac.uk

Citation:

Egan, J. V., Feng, W., James, A. D., Manners, J., Marsh, D. R., Lebonnois, S., et al. (2025). Is OSSO a significant contributor to the unknown UV absorber in Venus' atmosphere? *Geophysical Research Letters*, *52*, e2024GL113090. https://doi.org/10.1029/2024GL113090

Received 14 OCT 2024
Accepted 26 JAN 2025

Author Contributions:

Conceptualization: John M. C. Plane
Data curation: Joanna V. Egan
Formal analysis: Joanna V. Egan, John M. C. Plane
Funding acquisition: John M. C. Plane
Investigation: Joanna V. Egan
Project administration: John M. C. Plane
Software: Joanna V. Egan, Wuhu Feng, James Manners, Sébastien Lebonnois, Franck Lefèvre, Aurélien Stolzenbach
Supervision: Wuhu Feng, Alexander D. James, James Manners, Daniel R. Marsh, John M. C. Plane
Validation: Sébastien Lebonnois, Franck Lefèvre, Aurélien Stolzenbach
Writing – original draft: Joanna V. Egan, John M. C. Plane

1. Introduction

Patches of inhomogeneous near-UV (NUV) absorption were first observed in Venusian clouds in 1927 (Ross, 1928), and have since been extensively investigated (e.g., Molaverdikhani et al., 2012; Rossow et al., 1980; Titov et al., 2012; Travis et al., 1979; Yamazaki et al., 2018). Many candidates for the absorber have been proposed (see e.g., Titov et al. (2018)). Observed correlations with SO_2 may indicate that the absorber is a sulfur-containing species (Yamazaki et al., 2018), although the apparent correlation may arise from contributions from the unknown absorber at wavelengths generally assumed to correspond to SO_2 alone (Lee et al., 2021).

The combination of two isomers of the SO dimer (S_2O_2)—*cis*- and *trans*-OSSO, "OSSO" collectively—were proposed to be a significant contributor to the unknown UV absorption due to its ready formation from gas phase SO and good spectral agreement with the shape of the NUV absorber (Frandsen et al., 2016, 2020). Frandsen et al. (2016) predicted the formation of three isomers of S_2O_2 under Venusian conditions. Assuming equal production of *cis*- and *trans*-OSSO and modeling a photochemical steady state between formation from SO and destruction by photolysis, *cis*-OSSO would account for 69% of total S_2O_2, *trans*-OSSO 29%, and the remaining 2% cyclic-S_2O_2 (henceforth *cyc*-S_2O_2, the terminology is defined in Table S1 in Supporting Information S1). This result was supported by measurements of these species as the products of SO + SO combination in a matrix isolation experiment (Wu et al., 2018).

Writing – review & editing: Joanna V. Egan, Wuhu Feng, Alexander D. James, James Manners, Franck Lefèvre, John M. C. Plane

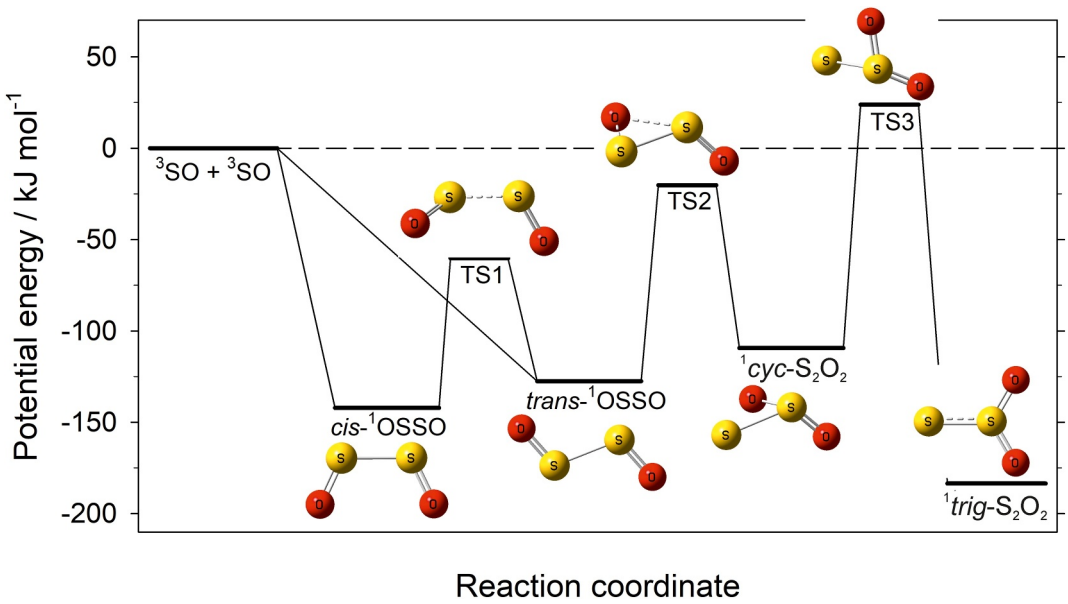

Figure 1. Potential energy surface (singlet spin multiplicity, zero-point energies included) for the reaction SO + SO (the triplet surface is not shown here to maintain clarity—see Figure S1 in Supporting Information S1). Calculations are at the w1bd level of theory (Barnes et al., 2009).

However, 1D photochemical modeling of the sulfur cycle in the Venusian atmosphere found that OSSO concentrations were two orders of magnitude too low to explain the observed UV absorption (Krasnopolsky, 2018; Pinto et al., 2021). Pinto et al. (2021) report modeled profiles for *cis*-OSSO, *trans*-OSSO and a fourth isomer, trigonal-S_2O_2 (henceforth *trig*-S_2O_2), with a peak concentration ratio of 64:16:20%, while Krasnopolsky (2018) reported a *cis*-OSSO:*trans*-OSSO ratio after photolysis of 82:18%, with no mention made of a third isomer. It should however be noted that Pinto et al. and Krasnopolsky both assume 70:30% production of the *cis*- and *trans*-isomers.

In this work, we revisit the reaction kinetics of the SO + SO reaction and investigate the kinetics of S_2O_2 with atomic O, which has been detected above the clouds, and Cl (Hübers et al., 2023). We then develop and use a whole atmosphere 3D model to predict the occurrence of the S_2O_2 isomers in Venus' atmosphere, and hence determine the resulting top-of-the-atmosphere (TOA) reflectance resulting from absorption by S_2O_2.

2. Modeling

2.1. Reaction Kinetics and Photochemistry

Rate coefficients for the reactions of SO and the S_2O_2 isomers were estimated by combining electronic structure (ab initio quantum theory) calculations with Rice-Ramsperger-Kassel-Markus (RRKM) statistical rate theory. The electronic structure calculations were carried out using the Gaussian 16 suite of programs (Frisch et al., 2016) to determine the nature of the potential energy surface (PES). The vibrational frequencies, rotational constants and energies of the stationary points (reactants, intermediates, transition states and products) of each reaction were calculated using the w1 Theory with Unrestricted Coupled Cluster and Brueckner Doubles (w1bd) method (Barnes et al., 2009; Frisch et al., 2016). The relative energies are consistent with those predicted by Hochlaf et al. (2021). The PES for SO + SO is illustrated in Figure 1. An RRKM calculation of the rate coefficients to form the S_2O_2 isomers was performed using the Master Equation Solver for Multi-Energy well Reactions (MESMER) program (Glowacki et al., 2012). See Supporting Information S1 for the vibrational frequencies and rotational constants of the stationary points (Table S2), and further details of the calculation (Georgievskii & Klippenstein, 2005; Gilbert & Smith, 1990). The resulting rate coefficients are listed in Table 1. The SO + SO reaction can also occur on a triplet surface. However, the initial triplet OSSO is weakly bound and there is a large barrier to forming triplet *trig*-S_2O_2 (Figure S1 in Supporting Information S1), so reaction on the triplet surface should not be an important source of S_2O_2.

Table 1
Reactions and Rate Coefficients Describing S_2O_2 Chemistry That Have Been Added to the PCM-Venus Model

No.	Reaction	Rate coefficient[a]
1	SO + SO (+CO_2) → *cis*-OSSO[b]	$k_0 = 3.85 \times 10^{-31}$ $(T/298)^{-3.36}$ $k_\infty = 1.1 \times 10^{-10}$ $(T/298)^{0.167}$ [c] $F_C = 0.42$
−1	*cis*-OSSO (+CO_2) → SO + SO	$k_1/(1.02 \times 10^{-27}$ exp(17231/T))
2	SO + SO (+CO_2) → *trans*-OSSO[b]	$k_0 = 2.82 \times 10^{-31}$ $(T/298)^{-3.38}$ $k_\infty = 1.1 \times 10^{-10}$ $(T/298)^{0.167}$ [c] $F_C = 0.42$
−2	*trans*-OSSO (+CO_2) → SO + SO	$k_2/(1.73 \times 10^{-27}$ exp(15395/T))
3	SO + SO (+CO_2) → *cyc*-S_2O_2[b]	$k_0 = 4.24 \times 10^{-32}$ $(T/298)^{-3.38}$ $k_\infty = 1.1 \times 10^{-10}$ $(T/298)^{0.167}$ [c] $F_C = 0.42$
−3	cyc-S_2O_2 (+CO_2) → SO + SO	$k_3/(6.75 \times 10^{-28}$ exp(13392/T))
4	*cis*-OSSO, *trans*-OSSO, and *cyc*-S_2O_2 + O → SO_2 + SO	1.1×10^{-10} $(T/298)^{0.167}$ [c]
5	*cis*-OSSO, *trans*-OSSO and *cyc*-S_2O_2 + Cl → ClSO + SO	1.1×10^{-10} $(T/298)^{0.167}$ [c]
6	ClSO + O → Cl + SO_2	1.1×10^{-10} $(T/298)^{0.167}$ [c]
Photolysis reactions		
7	*J*(*cis*-OSSO)	0.11
8	*J*(*trans*-OSSO)	0.23
9	*J*(*cyc*-S_2O_2)	9.5×10^{-3}
10	*J*(ClSO)	0.11

[a]Units: photolysis reactions, s^{-1}; bimolecular reactions, cm^3 $molecule^{-1}$ s^{-1}; termolecular, cm^6 $molecule^{-2}$ s^{-1}. See Supporting Information S1 for a detailed description of how these rate coefficients were calculated or estimated. [b]For recombination reactions the low pressure and high pressure limiting rate coefficients and the broadening factor (F_c) are defined in Burkholder et al. (2019). [c]Set to a hard-sphere collision rate coefficient typical for a barrierless reaction.

The optical absorption cross-sections of the relevant S_2O_2 isomers and ClSO were calculated using EOM-CCSD theory (Goings et al., 2014) with the aug-cc-pVQZ basis set (Frisch et al., 2016), for the first 30 excited electronic states for each molecule. The resulting spectra are illustrated in Figure S5 in Supporting Information S1. Each cross-section was then convolved up to its dissociation threshold with the solar actinic flux from the SOLAR2000 empirical solar irradiance model (Tobiska et al., 2000), scaled to Venus' orbit. The resulting photodissociation reactions are listed in Table 1. These TOA rates were fixed at all levels in the PCM-Venus model (during daytime); this is a reasonable approximation above 60 km where OSSO is abundant, since most of the photolysis occurs in spectral bands at wavelengths greater than 200 nm where attenuation of incoming solar radiation by CO_2 absorption is not significant.

Inspection of Figure 1 indicates that singlet *cis*-OSSO, *trans*-OSSO and *cyc*-S_2O_2 will be produced at temperatures below 350 K (i.e., pertinent to the upper clouds of Venus), with *cis*-OSSO being the major product because it is the most stable of these isomers and they are connected by submerged barriers TS1 and TS2. The most stable isomer, *trig*-S_2O_2, is not accessible at low temperatures because of the 23.3 kJ mol^{-1} barrier above the entrance channel (TS3).

A full list of all sulfur chemistry in the PCM can be found in Table S3, with a summary of changes to existing rate coefficients in Table S4. Besides thermal dissociation and photolysis, the OSSO isomers could also react with SO, CO, O, and Cl, which are all relatively abundant above 70 km. Reaction of OSSO with SO can only occur on a triplet surface and was found to have a large barrier, so is not considered further. The PES for reactions with CO, O, and Cl are shown in Figures S3–S5 in Supporting Information S1. Although the reaction of OSSO with CO is quite exothermic ($\Delta H_r^o(0\ K) = -203$ kJ mol^{-1}), the reaction has a pronounced barrier of 155 kJ mol^{-1}. Reaction of OSSO with O can either produced SSO + O_2, or SO_2 + SO. The first of these channels was explored in a recent

paper by Francés-Monerris et al. (2022) as a route to making poly-sulfur. However, there is a substantial barrier of 68 kJ mol^{-1} which will shut down this channel at low temperatures (Figure S3 in Supporting Information S1); instead, the products SO_2 + SO should form through a highly exothermic channel ($\Delta H_r^o(0\ K) = -404$ kJ mol^{-1}). Atomic Cl should react rapidly with OSSO to form ClSO + SO with no barrier ($\Delta H_r^o(0\ K) = -88$ kJ mol^{-1}) (Figure S4 in Supporting Information S1). The rate coefficients for these last two reactions were therefore assigned a value close to the collision capture rate, with a small T dependence (Table 1).

2.2. 3D Photochemical Modeling

3D modeling is performed using the Venus Planetary Climate Model (PCM) with photochemistry (Lebonnois et al., 2010; Stolzenbach et al., 2023). The horizontal grid has 96 latitude and 96 longitude bands (horizontal grid size of 1.875° × 3.75°). The model is run with 78 pressure levels from the surface (9.2×10^6 Pa) to 3.3×10^{-6} Pa (180 km). The PCM previously included S_2O_2 chemistry, but like other previous models (e.g., Krasnopolsky, 2016) treated all S_2O_2 present as the most stable isomer, *trig*-S_2O_2. Consideration of the potential energy surface of the SO + SO reaction finds (in agreement with Frandsen et al. (2016), Krasnopolsky (2018), and Pinto et al. (2021)) that this is not the case. This *trig*-S_2O_2 chemistry is therefore removed and replaced by the detailed chemistry of *cis*-OSSO, *trans*-OSSO, and *cyc*-S_2O_2.

The ablation of cosmic dust injects atomic sulfur into the atmosphere between ∼100 and 125 km peaking at 115 km, well below the homopause (Carrillo-Sánchez et al., 2020). The meteoric sulfur flux is calculated by scaling the modeled Na flux using mass abundances of 4.12% S and 0.47% Na, which are the weighted averages of different meteoritic groups (Gómez Martín et al., 2017). The ablated sulfur atoms enter the atmosphere at hyperthermal speeds, stripping O from CO_2 to produce SO (Gómez Martín et al., 2017).

2.3. Radiative Transfer Modeling

High resolution spectra were generated using a separate radiative transfer model for comparison to observations from the MASCS spectrometer on the MESSENGER spacecraft (Pérez-Hoyos et al., 2018). Radiative transfer modeling was performed using the SOCRATES (Suite Of Community Radiative Transfer codes based on Edwards and Slingo) 1D multiple scattering radiative transfer code developed by the UK Met Office (Manners et al., 2022a, 2022b). While SOCRATES has previously been developed to model Mars (McCulloch et al., 2023) and exoplanets (e.g., Boutle et al., 2020; Eager-Nash et al., 2020), this is the first time SOCRATES has been modified to model Venus. SOCRATES uses the two-stream approximation and correlated-k method to treat absorption (Edwards & Slingo, 1996; Goody et al., 1989). It has 78 pressure levels from the surface to 180 km (henceforth TOA) and 5 nm-wide spectral bands from 300 nm (the lower limit of MASCS observations) to 700 nm.

Due to the 300 nm lower limit, SO_2 is the only UV-absorbing gas modeled, other than the S_2O_2 isomers. While SOCRATES can model different atmospheric conditions, comparisons to MESSENGER are made with PCM results from equatorial regions, near midday, with a zenith angle of 52° and a surface albedo of 0.1. SOCRATES is initialized with the pressure, temperature, and gas and cloud mixing ratios from each level of the PCM. Aerosol scattering and absorption coefficients are calculated for 75 wt% sulfuric acid using Mie theory for each cloud mode (Knollenberg & Hunten, 1980). SO_2 UV absorption cross-section data is from HITRAN 2020 (Gordon et al., 2022), and the S_2O_2 isomer cross-sections were calculated (Section 2.1).

3. Results

3.1. Key Sulfur-Containing Species Concentrations

PCM-Venus was run for 9.0 Venus days (1050.75 Earth days) to reach steady state, with the chemistry and meteoric ablation of SO as described in Section 2.2. Figure 2 shows model profiles of SO_2 and SO compared to observations (Belyaev et al., 2012; Bertaux et al., 1996; Bézard et al., 1993; Encrenaz et al., 2012; Gel'man et al., 1979; Jessup et al., 2015; Krasnopolsky, 2010; Mahieux et al., 2023; Marcq et al., 2008; Na et al., 1994; Oyama et al., 1980; Sandor et al., 2010).

SO_2 was initialized at 10 ppm near the surface, and maintains a near-constant mixing ratio from the surface to the upper cloud layer (up to 60 km). This is more than an order of magnitude lower than observations of the below-cloud region, which consistently report 150 ppm SO_2 near the surface (Bertaux et al., 1996; Bézard et al., 1993;

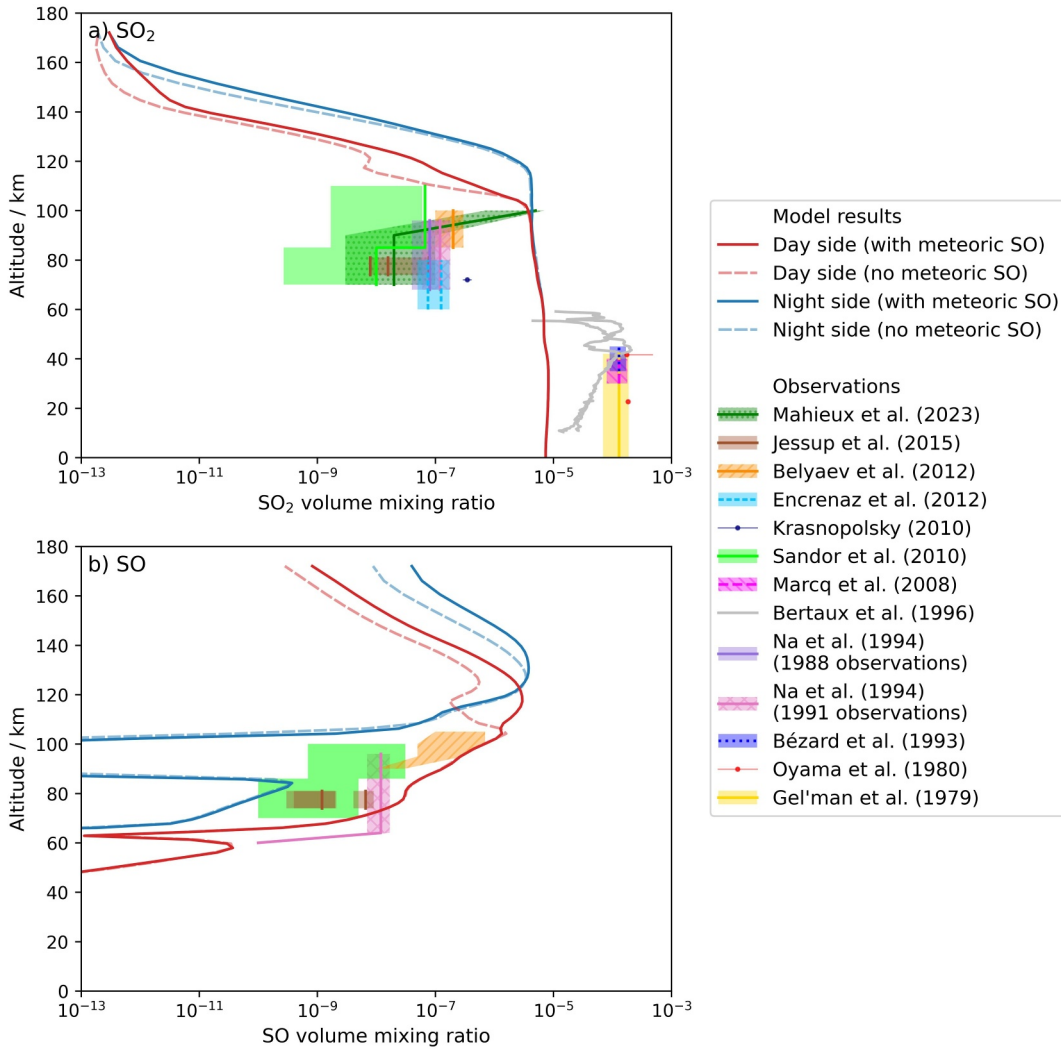

Figure 2. Comparison of (a) SO_2 and (b) SO mixing ratio to observations. Model results are averaged from −30° to 30° latitude. Dayside (nightside) is defined as the 140° longitude centered on the subsolar (antisolar) point to prevent capturing terminators. SO dayside (red) profiles are toward the upper limit of or just above observations. SO_2 profiles are an order of magnitude too low below the clouds and ∼3 orders of magnitude too high above the clouds.

Gel'man et al., 1979; Marcq et al., 2008; Oyama et al., 1980). It is clear that a significant sulfur reservoir in the cloud layer is missing from photochemical modeling of Venus (Vandaele et al., 2017, and references therein), resulting in a negligible decrease in modeled SO_2 through the clouds. Recognizing this as a significant unsolved problem for Venusian research, we chose a compromise value that under-estimates below-cloud observations, but still overestimates above-cloud observations (Figure 2). This also demonstrates that S_2O_2 does not provide a significant above-cloud sulfur reservoir. We then make no further attempt to constrain the above-cloud SO_2 concentration to observed levels, thereby maximizing the possible OSSO concentration.

On the dayside of the planet, SO is primarily produced by photolysis of SO_2 into SO and O. On both sides of the planet, injection of SO by the ablation of cosmic dust contributes a modeled flux of 3.2 tonnes per Earth day, peaking at 115 km (Carrillo-Sánchez et al., 2020; Gómez Martín et al., 2017). In Figure 2, the lack of photolytically produced SO on the nightside is apparent as a sharp decrease in concentration at 90–110 km, while the SO peak above 110 km is maintained by meteoric input and transport. The effect of photolysis below 100 km is not apparent in the SO_2 profile due to the log scale.

S_2O_2 is most abundant in a thin layer (note 12 orders of magnitude across the log scale) near 70 km (Figure 3). Higher concentrations of S_2O_2 occur on the night side of the planet, by an order of magnitude near the peak of the

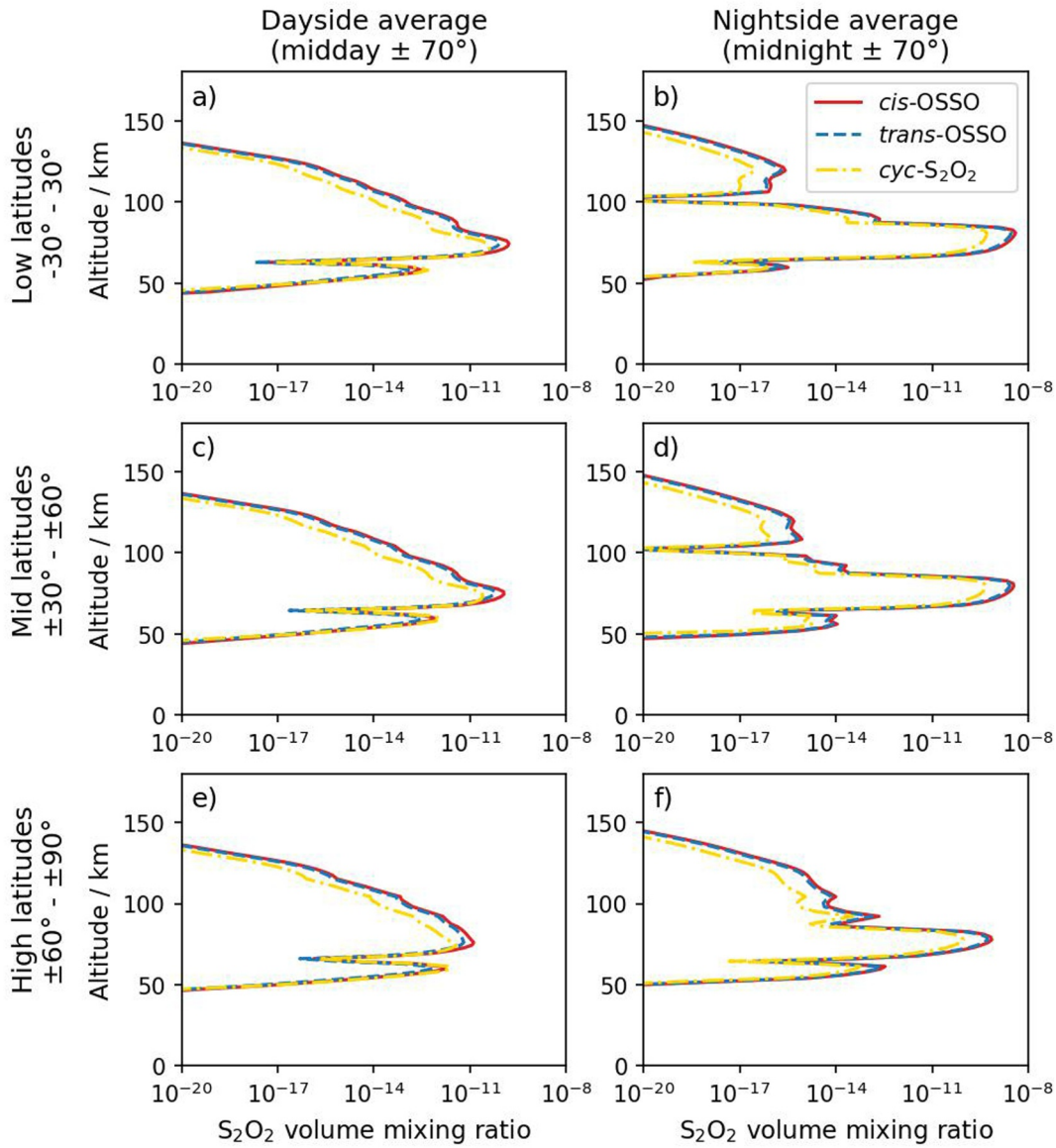

Figure 3. Mixing ratio profiles of the three S_2O_2 isomers in different latitude bands and local times. An average is taken across 140° centered on the subsolar or antisolar points to avoid capturing the terminators in dayside and nightside averages, respectively.

absorption, with a slight decrease in peak concentration from low to high latitudes. The decrease in nightside S_2O_2 concentration near 100 km reflects a decrease in production because of reduced SO, rather than an increase in the S_2O_2 loss rate. A 2D colormap of S_2O_2 column abundance above 60 km is shown in Figure S6 in Supporting Information S1, illustrating the high concentrations on the night side. The dominant form of S_2O_2 is *cis*-OSSO at all altitudes above ~60 km, followed by *trans*-OSSO and then *cyc*-S_2O_2, in the ratio 57:34:9% at the dayside peak. In the 50–60 km region where photolysis dominates the loss of S_2O_2, the cyclic form becomes the dominant isomer due to its longer lifetime against photolysis (Table 1).

Dayside production and loss, and the dominance of the different loss processes with altitude are shown in Figure S7 in Supporting Information S1. The higher peak S_2O_2 concentration at 60–80 km at night is attributed to the lack of photolysis on the night side, as it is the dominant loss mechanism in this region on the dayside. The primary loss mechanism above 70 km on the dayside and above 60 km on the night side is reaction with atomic O to produce SO_2 and SO. Below 40 km, thermal decomposition of S_2O_2 following collision with a third body (assumed to be

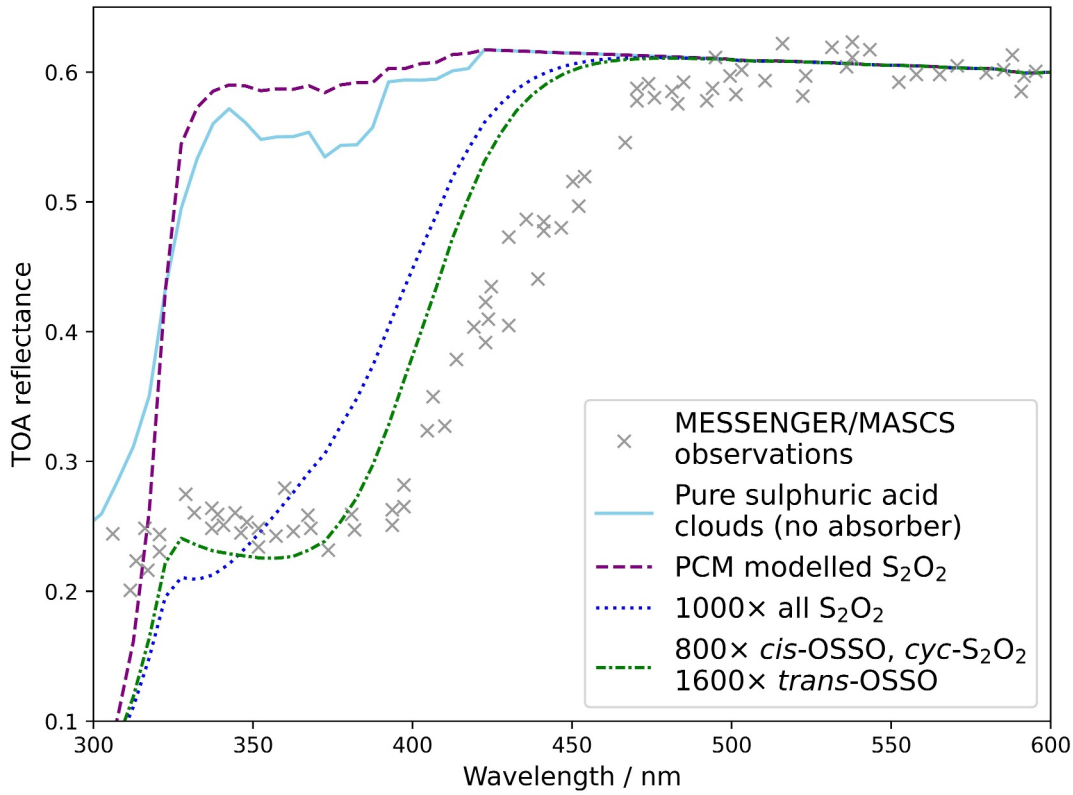

Figure 4. SOCRATES modeled TOA reflectance for the PCM concentrations of OSSO and various scaling factors (see the text for further details).

CO_2) dominates the loss. Loss of S_2O_2 by reaction with atomic chlorine is never dominant on the day side as the Cl concentration is much lower than O in and above the cloud layer. Reaction with Cl becomes faster than O below the clouds, but S_2O_2 destruction in this region is dominated by thermal decomposition. O and Cl destruction are comparable in the photolytically dominated region on the dayside and both contribute on the nightside.

3.2. Modeled Reflectance

Using the Venus-PCM results after 9.0 Venus days, the TOA reflectance computed using SOCRATES (purple, dashed line) is presented in Figure 4. The deep absorption shortwards of 320 nm is due to SO_2, which is significantly overestimated by the PCM in this run (see Section 3.1). Higher absorption in the 320–400 nm range for the case with no absorber and a constructed SO_2 profile in line with observations (light blue, solid) compared to the PCM concentrations is attributed to the higher SO_2 concentrations below the clouds in observations. The PCM-modeled S_2O_2 concentrations are clearly insufficient to reproduce the strength of the NUV absorption observed by MESSENGER (gray crosses, Pérez-Hoyos et al. (2018)).

We estimate the approximate scale of the deficit in S_2O_2 by scaling the concentration profiles and find that an increase of ∼3 orders of magnitude (dark blue, dotted) is required in OSSO concentration to reach reflectance of 0.2–0.3 in the near-UV. However, note the poor agreement of the shape of the absorption spectrum, producing a significantly narrower absorption region than observed. A broader absorption feature can be produced by increasing the ratio of *trans*-OSSO to *cis*-OSSO by a factor of 2 (green, dash-dotted), though note that the agreement with observations remains poor, particularly from 400 to 500 nm. Moreover, there is no justification in terms of the reaction kinetics for *trans*-OSSO being the dominant isomer, which all previous studies agreed is not the case. The *cyc*-S_2O_2 is, in all cases, scaled by the same factor as the *cis*-OSSO, and contributes negligibly to the observed absorption (Figure S8 in Supporting Information S1).

For direct comparison to previous work, which did not include S_2O_2 reaction with O and/or Cl as a possible loss mechanism (Frandsen et al., 2016; Krasnopolsky, 2018; Pinto et al., 2021), we investigate the sensitivity of the OSSO concentrations to these reactions. Although examination of the PESs of the reactions of O and Cl with OSSO indicates no energy barriers with respect to the reaction entrance channels, and hence are assigned nominal capture rate coefficients (Table 1), we performed a sensitivity analysis by considering two test cases: (1) decreasing the rate coefficients by a factor of 100, and (2) removing the O and Cl reactions as loss processes for S_2O_2. For test 1, the peak OSSO concentrations increase by factors of 4.0 and 2.9 for *cis*- and *trans*-OSSO, respectively. For test 2, *cis*- and *trans*-OSSO increase by factors of 4.1 and 2.9 (Figure S9 in Supporting Information S1). The majority of the changes in OSSO concentrations occur above 80 km where reaction with O is the dominant loss mechanism. For both cases, the agreement with the spectral shape of the Venusian absorber is worse due to a decrease in the fraction of *trans*-OSSO, and the resulting OSSO concentrations are too low to match observations by two orders of magnitude (Figure S10 in Supporting Information S1), in agreement with Krasnopolsky (2018) and Pinto et al. (2021).

4. Conclusions

We present here an updated sulfur chemistry network in the PCM-Venus model for three forms of S_2O_2: *cis*-OSSO, *trans*-OSSO, and *cyc*-S_2O_2. We include meteoric ablation injection of SO above 100 km, and allow the model to run to steady-state, increasing the cloud-level SO_2 significantly above observed levels to produce the highest SO and therefore OSSO concentrations achievable. We find that S_2O_2 cannot provide the missing sulfur reservoir in the cloud deck required to explain SO_2 observations.

The concentrations of S_2O_2 produced by the model result in a 57:34:9% ratio of *cis*-OSSO:*trans*-OSSO:*cyc*-S_2O_2 and have no observable effect on the TOA reflectance as modeled by SOCRATES, a 1D multiple scattering radiative transfer model. The dominant loss mechanism of S_2O_2 is found to be reaction with O above ∼70 km, thermal decomposition below 40 km, and photolysis (on the dayside) or reaction with O and Cl (on the nightside) from 40 to 70 km. Using this chemistry scheme, the OSSO concentrations are approximately three orders of magnitude too low to explain the observed absorbance, and the spectral shape of the absorption shows poor agreement with that of the unknown absorber. To improve the agreement of the spectral shape, a further factor of two increase in *trans*-OSSO is required. If loss of OSSO with O and Cl is discounted, the OSSO concentration increases, but is still two orders of magnitude lower than required to explain the absorption, and maintains poor agreement with the spectral shape observed.

We therefore conclude that OSSO does not make a significant contribution to the Venusian UV absorption.

Data Availability Statement

Data for the theoretical calculations and figures is listed in Supporting Information S1. Other data plotted in the figures, and PCM-Venus and SOCRATES model output are available (Egan et al., 2024).

Acknowledgments
We thank the UK Science and Technology Research Council for funding this study (project ST/T000279/1). JVE acknowledges funding for a PhD studentship from the UK Engineering and Physical Sciences Research Council through the Center for Doctoral Training in Aerosol Science (EP/S023593/1).

References

Barnes, E. C., Petersson, G. A., Montgomery, J. A., Frisch, M. J., & Martin, J. M. L. (2009). Unrestricted coupled cluster and brueckner doubles variations of W1 theory. *Journal of Chemical Theory and Computation*, *5*(10), 2687–2693. https://doi.org/10.1021/ct900260g

Belyaev, D. A., Montmessin, F., Bertaux, J.-L., Mahieux, A., Fedorova, A. A., Korablev, O. I., et al. (2012). Vertical profiling of SO_2 and SO above Venus' clouds by SPICAV/SOIR solar occultations. *Icarus*, *217*(2), 740–751. https://doi.org/10.1016/j.icarus.2011.09.025

Bertaux, J.-L., Widemann, T., Hauchecorne, A., Moroz, V. I., & Ekonomov, A. P. (1996). VEGA 1 and VEGA 2 entry probes: An investigation of local UV absorption (220–400 nm) in the atmosphere of Venus (SO_2 aerosols, cloud structure). *Journal of Geophysical Research*, *101*(E5), 12709–12745. https://doi.org/10.1029/96JE00466

Bézard, B., Bergh, C., Fegley, B., Maillard, J.-P., Crisp, D., Owen, T., et al. (1993). The abundance of sulfur dioxide below the clouds of Venus. *Geophysical Research Letters*, *20*(15), 1587–1590. https://doi.org/10.1029/93GL01338

Boutle, I. A., Joshi, M., Lambert, F. H., Mayne, N. J., Lyster, D., Manners, J., et al. (2020). Mineral dust increases the habitability of terrestrial planets but confounds biomarker detection. *Nature Communications*, *11*(1), 2731. https://doi.org/10.1038/s41467-020-16543-8

Burkholder, J. B., Sander, S. P., Abbatt, J., Barker, J. R., Cappa, C., Crounse, J. D., et al. (2019). *Chemical kinetics and photochemical data for use in atmospheric studies, evaluation no. 19*. Jet Propulsion Laboratory.

Carrillo-Sánchez, J. D., Gómez-Martín, J. C., Bones, D. L., Nesvorný, D., Pokorný, P., Benna, M., et al. (2020). Cosmic dust fluxes in the atmospheres of Earth, Mars, and Venus. *Icarus*, *335*, 113395. https://doi.org/10.1016/j.icarus.2019.113395

Eager-Nash, J. K., Reichelt, D. J., Mayne, N. J., Hugo Lambert, F., Sergeev, D. E., Ridgway, R. J., et al. (2020). Implications of different stellar spectra for the climate of tidally locked Earth-like exoplanets. *Astronomy and Astrophysics*, *639*, A99. https://doi.org/10.1051/0004-6361/202038089

Edwards, J. M., & Slingo, A. (1996). Studies with a flexible new radiation code. I: Choosing a configuration for a large-scale model. *Quarterly Journal of the Royal Meteorological Society*, *122*(531), 689–719. https://doi.org/10.1002/qj.49712253107

Egan, J. V., Feng, W., James, A. D., Manners, J., Marsh, D. R., Lebonnois, S., et al. (2024). In J. V. Egan (Eds.), *Is OSSO a significant contributor to the unknown UV absorber in Venus' atmosphere?* [Dataset]. Zenodo - EU Open Research Repository. https://doi.org/10.5281/zenodo.13929706

Encrenaz, T., Greathouse, T. K., Roe, H., Richter, M., Lacy, J., Bézard, B., et al. (2012). HDO and SO_2 thermal mapping on Venus: Evidence for strong SO_2 variability. *Astronomy and Astrophysics*, *543*, A153. https://doi.org/10.1051/0004-6361/201219419

Francés-Monerris, A., Carmona-García, J., Trabelsi, T., Saiz-Lopez, A., Lyons, J. R., Francisco, J. S., & Roca-Sanjuán, D. (2022). Photochemical and thermochemical pathways to S_2 and polysulfur formation in the atmosphere of Venus. *Nature Communications*, *13*(1), 4425. https://doi.org/10.1038/s41467-022-32170-x

Frandsen, B. N., Farahani, S., Vogt, E., Lane, J. R., & Kjaergaard, H. G. (2020). Spectroscopy of OSSO and other sulfur compounds thought to be present in the Venus atmosphere. *The Journal of Physical Chemistry A*, *124*(35), 7047–7059. https://doi.org/10.1021/acs.jpca.0c04388

Frandsen, B. N., Wennberg, P. O., & Kjaergaard, H. G. (2016). Identification of OSSO as a near-UV absorber in the Venusian atmosphere. *Geophysical Research Letters*, *43*(21), 11146–111155. https://doi.org/10.1002/2016GL070916

Frisch, M. J., Trucks, G. W., Schlegel, H. B., Scuseria, G. E., Robb, M. A., Cheeseman, J. R., et al. (2016). *Gaussian 16 Rev. C.01*. Gaussian Inc.

Gel'man, B. G., Zolotukhin, V. G., Lamonivm, N. I., Levchuk, B. V., Mukhin, L. M., Nenarokov, D. F., et al. (1979). *Analiz khimicheskogo sostava atmosfery venery na AMS Venera-12 gazovym khromatografom*. NASA.

Georgievskii, Y., & Klippenstein, S. J. (2005). Long-range transition state theory. *Journal of Chemical Physics*, *122*(19), 194103. https://doi.org/10.1063/1.1899603

Gilbert, R. G., & Smith, S. C. (1990). *Theory of unimolecular and recombination reactions*. Blackwell.

Glowacki, D. R., Liang, C. H., Morley, C., Pilling, M. J., & Robertson, S. H. (2012). MESMER: An open-source master equation solver for multi-energy well reactions. *Journal of Physical Chemistry A*, *116*(38), 9545–9560. https://doi.org/10.1021/jp3051033

Goings, J., Caricato, M., Frisch, M. J., & Li, X. (2014). Assessment of low-scaling approximations to the equation of motion coupled-cluster singles and doubles equations. *Journal of Chemical Physics*, *141*(16), 164116. https://doi.org/10.1063/1.4898709

Gómez Martín, J. C., Brooke, J. S. A., Feng, W., Höpfner, M., Mills, M. J., & Plane, J. M. C. (2017). Impacts of meteoric sulfur in the Earth's atmosphere. *Journal of Geophysical Research: Atmospheres*, *122*(14), 7678–7701. https://doi.org/10.1002/2017JD027218

Goody, R., West, R., Chen, L., & Crisp, D. (1989). The correlated-k method for radiation calculations in nonhomogeneous atmospheres. *Journal of Quantitative Spectroscopy and Radiative Transfer*, *42*(6), 539–550. https://doi.org/10.1016/0022-4073(89)90044-7

Gordon, I. E., Rothman, L., Hargreaves, R., Hashemi, R., Karlovets, E., Skinner, F., et al. (2022). The HITRAN2020 molecular spectroscopic database. *Journal of Quantitative Spectroscopy and Radiative Transfer*, *277*, 107949. https://doi.org/10.1016/j.jqsrt.2021.107949

Hochlaf, M., Linguerri, R., Cheraki, M., Ayari, T., Ben Said, R., Feifel, R., & Chambaud, G. (2021). $S_2O_2^{q+}$ (q = 0, 1, and 2) molecular systems: Characterization and atmospheric planetary implications. *The Journal of Physical Chemistry A*, *125*(9), 1958–1971. https://doi.org/10.1021/acs.jpca.0c11407

Hübers, H.-W., Richter, H., Graf, U. U., Güsten, R., Klein, B., Stutzki, J., & Wiesemeyer, H. (2023). Direct detection of atomic oxygen on the dayside and nightside of Venus. *Nature Communications*, *14*(1), 6812. https://doi.org/10.1038/s41467-023-42389-x

Jessup, K. L., Marcq, E., Mills, F., Mahieux, A., Limaye, S., Wilson, C., et al. (2015). Coordinated hubble space telescope and Venus express observations of Venus' upper cloud deck. *Icarus*, *258*, 309–336. https://doi.org/10.1016/j.icarus.2015.05.027

Knollenberg, R. G., & Hunten, D. M. (1980). The microphysics of the clouds of Venus: Results of the Pioneer Venus particle size spectrometer experiment. *Journal of Geophysical Research*, *85*(A13), 8039–8058. https://doi.org/10.1029/JA085iA13p08039

Krasnopolsky, V. A. (2010). Spatially-resolved high-resolution spectroscopy of Venus 2. Variations of HDO, OCS, and SO_2 at the cloud tops. *Icarus*, *209*(2), 314–322. https://doi.org/10.1016/j.icarus.2010.05.008

Krasnopolsky, V. A. (2016). Sulfur aerosol in the clouds of Venus. *Icarus*, *274*, 33–36. https://doi.org/10.1016/j.icarus.2016.03.010

Krasnopolsky, V. A. (2018). Disulfur dioxide and its near-UV absorption in the photochemical model of Venus atmosphere. *Icarus*, *299*, 294–299. https://doi.org/10.1016/j.icarus.2017.08.013

Lebonnois, S., Hourdin, F., Eymet, V., Crespin, A., Fournier, R., & Forget, F. (2010). Superrotation of Venus' atmosphere analyzed with a full general circulation model. *Journal of Geophysical Research*, *115*(E6). https://doi.org/10.1029/2009JE003458

Lee, Y. J., García Muñoz, A., Yamazaki, A., Yamada, M., Watanabe, S., & Encrenaz, T. (2021). Investigation of UV absorbers on Venus using the 283 and 365 nm phase curves obtained from Akatsuki. *Geophysical Research Letters*, *48*(7), e2020GL090577. https://doi.org/10.1029/2020GL090577

Mahieux, A., Robert, S., Mills, F. P., Jessup, K. L., Trompet, L., Aoki, S., et al. (2023). Update on SO_2, detection of OCS, CS, CS_2, and SO_3, and upper limits of H_2S and HOCl in the Venus mesosphere using SOIR on board Venus Express. *Icarus*, *399*, 115556. https://doi.org/10.1016/j.icarus.2023.115556

Manners, J., Edwards, J. M., Hill, P., & Thelen, J.-C. (2022a). *SOCRATES technical guide*. UK Met Office.

Manners, J., Edwards, J. M., Hill, P., & Thelen, J.-C. (2022b). *SOCRATES user guide*. UK Met Office.

Marcq, E., Bézard, B., Drossart, P., Piccioni, G., Reess, J. M., & Henry, F. (2008). A latitudinal survey of CO, OCS, H_2O, and SO_2 in the lower atmosphere of Venus: Spectroscopic studies using VIRTIS-H. *Journal of Geophysical Research*, *113*(E5). https://doi.org/10.1029/2008JE003074

McCulloch, D., Sergeev, D. E., Mayne, N., Bate, M., Manners, J., Boutle, I., et al. (2023). A modern-day Mars climate in the Met Office Unified model: Dry simulations. *Geoscientific Model Development*, *16*(2), 621–657. https://doi.org/10.5194/gmd-16-621-2023

Molaverdikhani, K., McGouldrick, K., & Esposito, L. W. (2012). The abundance and vertical distribution of the unknown ultraviolet absorber in the Venusian atmosphere from analysis of Venus Monitoring Camera images. *Icarus*, *217*(2), 648–660. https://doi.org/10.1016/j.icarus.2011.08.008

Na, C. Y., Esposito, L. W., McClintock, W. E., & Barth, C. A. (1994). Sulfur dioxide in the atmosphere of Venus: II. Modeling results. *Icarus*, *112*(2), 389–395. https://doi.org/10.1006/icar.1994.1193

Oyama, V. I., Carle, G. C., Woeller, F., Pollack, J. B., Reynolds, R. T., & Craig, R. A. (1980). Pioneer Venus gas chromatography of the lower atmosphere of Venus. *Journal of Geophysical Research*, *85*(A13), 7891–7902. https://doi.org/10.1029/JA085iA13p07891

Pérez-Hoyos, S., Sánchez-Lavega, A., García-Muñoz, A., Irwin, P. G. J., Peralta, J., Holsclaw, G., et al. (2018). Venus upper clouds and the UV absorber from MESSENGER/MASCS observations. *Journal of Geophysical Research: Planets*, *123*(1), 145–162. https://doi.org/10.1002/2017JE005406

Pinto, J. P., Li, J., Mills, F. P., Marcq, E., Evdokimova, D., Belyaev, D., & Yung, Y. L. (2021). Sulfur monoxide dimer chemistry as a possible source of polysulfur in the upper atmosphere of Venus. *Nature Communications*, *12*(1), 175. https://doi.org/10.1038/s41467-020-20451-2

Ross, F. E. (1928). Photographs of Venus. *The Astrophysical Journal*, *68*, 57. https://doi.org/10.1086/143130

Rossow, W. B., Del Genio, A. D., Limaye, S. S., Travis, L. D., & Stone, P. H. (1980). Cloud morphology and motions from Pioneer Venus images. *Journal of Geophysical Research*, *85*(A13), 8107–8128. https://doi.org/10.1029/JA085iA13p08107

Sandor, B. J., Todd Clancy, R., Moriarty-Schieven, G., & Mills, F. P. (2010). Sulfur chemistry in the Venus mesosphere from SO_2 and SO microwave spectra. *Icarus*, *208*(1), 49–60. https://doi.org/10.1016/j.icarus.2010.02.013

Stolzenbach, A., Lefèvre, F., Lebonnois, S., & Määttänen, A. (2023). Three-dimensional modeling of Venus photochemistry and clouds. *Icarus*, *395*, 115447. https://doi.org/10.1016/j.icarus.2023.115447

Titov, D. V., Ignatiev, N. I., McGouldrick, K., Wilquet, V., & Wilson, C. F. (2018). Clouds and hazes of Venus. *Space Science Reviews*, *214*(8), 126. https://doi.org/10.1007/s11214-018-0552-z

Titov, D. V., Markiewicz, W. J., Ignatiev, N. I., Song, L., Limaye, S. S., Sanchez-Lavega, A., et al. (2012). Morphology of the cloud tops as observed by the Venus express monitoring camera. *Icarus*, *217*(2), 682–701. https://doi.org/10.1016/j.icarus.2011.06.020

Tobiska, W. K., Woods, T., Eparvier, F., Viereck, R., Floyd, L., Bouwer, D., et al. (2000). The SOLAR2000 empirical solar irradiance model and forecast tool. *Journal of Atmospheric and Solar-Terrestrial Physics*, *62*(14), 1233–1250. https://doi.org/10.1016/S1364-6826(00)00070-5

Travis, L. D., Coffeen, D. L., Genio, A. D. D., Hansen, J. E., Kawabata, K., Lacis, A. A., et al. (1979). Cloud images from the Pioneer Venus orbiter. *Science*, *205*(4401), 74–76. https://doi.org/10.1126/science.205.4401.74

Vandaele, A. C., Korablev, O., Belyaev, D., Chamberlain, S., Evdokimova, D., Encrenaz, T., et al. (2017). Sulfur dioxide in the Venus atmosphere: I. Vertical distribution and variability. *Icarus*, *295*, 16–33. https://doi.org/10.1016/j.icarus.2017.05.003

Wu, Z., Wan, H., Xu, J., Lu, B., Lu, Y., Eckhardt, A. K., et al. (2018). The near-UV absorber OSSO and its isomers. *Chemical Communications*, *54*(36), 4517–4520. https://doi.org/10.1039/C8CC00999F

Yamazaki, A., Yamada, M., Lee, Y. J., Watanabe, S., Horinouchi, T., Murakami, S. Y., et al. (2018). Ultraviolet imager on Venus orbiter Akatsuki and its initial results. *Earth Planets and Space*, *70*(1), 23. https://doi.org/10.1186/s40623-017-0772-6